Influence of band structure on the large thermoelectric performance of lanthanum telluride

Andrew F. May,[1] David J. Singh,[2] and G. Jeffrey Snyder[3]
[1]*Department of Chemical Engineering, California Institute of Technology, Pasadena, California 91125, USA*
[2]*Materials Science and Technology Division, Oak Ridge National Laboratory, Oak Ridge, Tennessee 37831-6114, USA*
[3]*Department of Materials Science, California Institute of Technology, Pasadena, California 91125, USA*
(Received 5 February 2009; published 1 April 2009)

We investigate the carrier density and temperature dependence of the Seebeck coefficient of $La_{3-x}Te_4$ via density-functional calculations and Boltzmann transport theory. The pertinent band structure has light bands at the band gap and heavy degenerate bands with band minima near energies corresponding to the experimentally determined optimum carrier density. Heavy bands increase the energy dependence of the density of states, which increases the magnitude of the Seebeck coefficient in an itinerant conduction regime, while the light bands provide a conduction channel that works against carrier localization promoted by La vacancies. The net result is thermoelectric performance greater than current *n*-type materials above 1000 K.

DOI: 10.1103/PhysRevB.79.153101 PACS number(s): 72.15.Jf, 71.20.Nr, 71.15.Mb

I. INTRODUCTION

Thermoelectric materials are used to convert between thermal and electrical energies via the solid state. Materials capable of making an efficient thermoelectric converter must possess a low thermal conductivity (κ) and large magnitudes of the electrical conductivity (σ) and Seebeck coefficient (α). These transport properties combine to form the dimensionless figure of merit $zT=\alpha^2\sigma T/\kappa$, which quantifies the maximum thermoelectric efficiency of a material. However, the relevant electrical transport quantities typically have opposing dependences on carrier concentration (n) and temperature (T), greatly complicating the search for high-zT materials.

In a single parabolic band (SPB) semiconductor, the highest zT is typically obtained at doping levels corresponding to an electrochemical potential (E_F) positioned slightly above the minimum conduction energy (for *n*-type). This is primarily the result of a balance between α and σ: α is largest when E_F is near the band minimum, but the corresponding value of σ is typically small due to low n ($\sigma=ne\mu$, where μ=mobility). Furthermore, itinerant conduction is not always obtained at such doping levels and a decrease in μ associated with localization may be observed. This is especially the case in heavy band systems. In fact, electron localization is of particular concern for $Re_{3-x}X_4$ compounds (Re =rare earth and X=chalcogenide), which, at low carrier concentrations, contain a large number of randomly distributed cation vacancies that promote Anderson localization.[1]

The Seebeck coefficient is large near the band edge because it is proportional to the logarithmic derivative of the conductivity (explicitly at low T). This behavior can be expressed via

$$\alpha = \frac{\pi^2 k_b^2 T}{3q}\left(\frac{d\ln N(E)}{dE} + \frac{d\ln \tau(E)v(E)^2}{dE}\right)_{E=E_F}. \quad (1)$$

Equation (1) is one representation of the Mott relation, which is the low T limit for α of a single-band metal. This formula is generated by employing $\sigma \propto Nv^2\tau$, where $N(E)$ is the density of states and $\tau(E)$ and $v(E)$ are the relaxation time and average electron velocity, respectively.[2] While the Mott formula is the low-T limit, the more general expressions utilized here for finite T also have similar behavior. Band features such as degeneracy (g_i) and effective mass (m_i^*) impact the balance between α and σ, and large g_i and m_i^* are desirable for thermoelectric materials.[3] Ideally, the large α associated with a band edge would be combined with the σ associated with an itinerant band containing large n (hence the desire for large m^*). It is possible to increase $|\alpha|$ at a given n by increasing the energy dependence of $N(E)$, for instance, via resonant states as demonstrated in Tl-doped PbTe by Heremans *et al.*[4] Similar behavior has been proposed in the LAST $[(PbTe)_{1-x}(AgSbTe_2)_x]$ system by Bilc *et al.*[5] In such systems, the potential role of band-structure calculations is evident. In general, first-principles calculations help provide greater understanding of the physics governing electronic transport and are thus an invaluable tool in the field of thermoelectricity.

$La_{3-x}Te_4$ is capable of $zT\sim 1.2$ near 1300 K, making it the highest performing bulk *n*-type material above 1000 K—an important range for power generation and deep space application. The optimum carrier concentration is $n\sim 9\times 10^{20}$ cm^{-3} and the large zT is due to a relatively large $|\alpha|$ at high n, as well as a low lattice thermal conductivity. A single parabolic band model yields relatively large effective masses ($m^*=2-4m_e$), is incapable of describing the dependence of α on n for all values of n,[6,7] and makes it difficult to understand how a material with a high concentration of vacancies and a large effective mass is conducting. Isolating the basis of the deviation from single-band behavior is critical for developing a physical model of transport, which could guide future efforts to improve thermoelectric efficiency in this material class. Furthermore, the ability to examine the dependence of α on n in the absence of vacancies (via *ab initio* calculations) leads to unique insights about transport in $Re_{3-x}X_4$.

II. METHODS

The electronic structure of cubic La_3Te_4 was calculated within the local-density approximation (LDA) using the linearized augmented plane-wave (LAPW) method with local

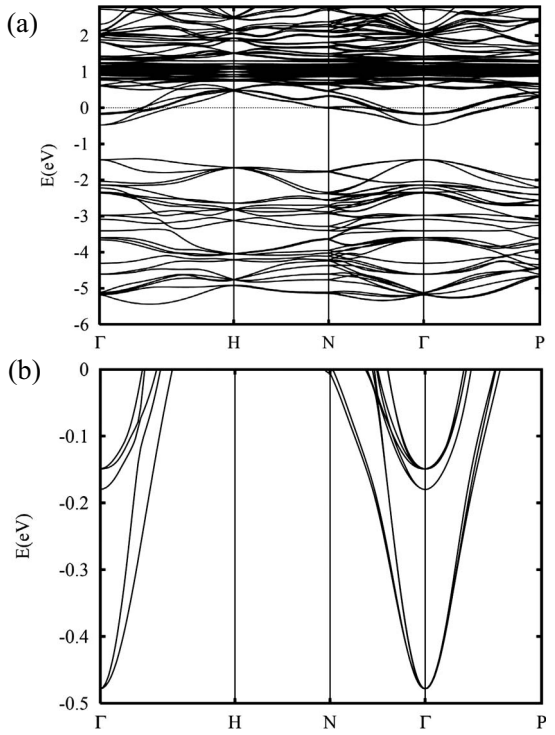

FIG. 1. Electronic band structure for La_3Te_4 for (a) large energy scale and (b) energy of pertinent conduction bands with $E_F=0$. The band minima are found to be nearly parabolic, with band mass and degeneracy noted in the text.

orbitals[8] as implemented in WIEN2K.[9] The experimental lattice parameter of $a=9.634$ Å from Ref. 10 was used with LAPW sphere radii of 2.9 bohr and tested basis sets. Relativistic effects, including spin orbit, were included. While calculations of transport properties require knowledge regarding the relevant scattering mechanisms, the Hall and Seebeck coefficients do not contain a dimension of time and can often be well characterized by assuming that the electronic relaxation time (τ) is independent of energy. Here, we call this the constant relaxation time approximation (CRTA), which is generally valid when the pertinent bands are associated with similar bonding. The Boltzmann transport equation was utilized to calculate the Seebeck and Hall coefficients within the CTRA using the BOLTZTRAP code.[11] Experimental results of α, σ, and κ discussed here were presented as a function of n and T by May *et al.*[7]

III. RESULTS AND DISCUSSION

The calculated band structure [Figs. 1(a) and 1(b)] for La_3Te_4 has a direct gap at Γ of 0.95 eV. The insulating composition corresponds to $La_{3-x}Te_4$ with $x=1/3$ (stoichiometry La_2Te_3) and electrons fill conduction states as La vacancies are filled. At full lanthanum occupancy (La_3Te_4), there is one free electron per formula unit (e^-/f.u.) and the corresponding Fermi energy $E_F=0.48$ eV above the conduction-band edge. We start with rigid bands and vary E_F to probe the n dependence of α. Therefore, within the limits of this assumption, we can examine the behavior of α in *vacancy-free* $La_{3-x}Te_4$, which is impossible do experimentally.

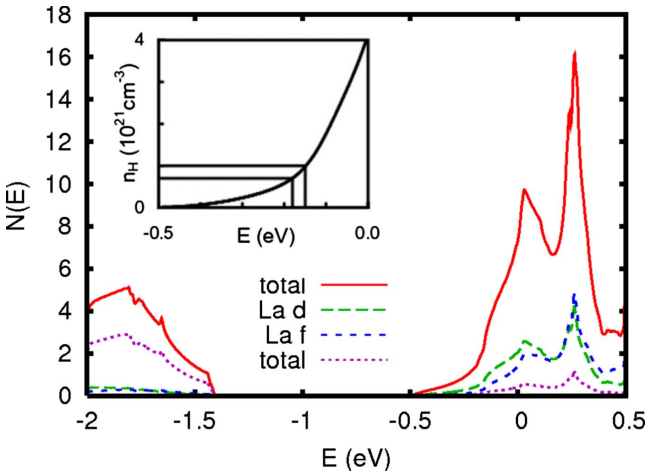

FIG. 2. (Color online) The density of states $N(E)$ demonstrates a sharp increase near −0.16 eV due to the presence of heavy bands. This behavior is similarly reflected in the inset, which shows the Hall carrier concentration at 300 K in units of 10^{21} cm^{-3}. Solid lines indicate the location of the heavy band minima, which correspond to the optimum doping level.

The band structure is given in Fig. 1, with the pertinent bands for electron conduction in the lower panel. The energy minima of these bands are $E_{\min,1}=-0.48$ eV, $E_{\min,2}=-0.18$ eV, and $E_{\min,3}=-0.15$ eV (relative to E_F). The two higher-energy bands would be degenerate at Γ in the absence of spin orbit. We obtain parabolic band effective masses of $m_1^*/m_e=0.39$, $m_2^*/m_e=1.05$, and $m_3^*/m_e=1.56$. The corresponding degeneracy for each band is $g_1=2$, $g_2=1$, and $g_3=2$, where spin degeneracy is not included. Figure 2 shows the electronic density of states and projections. It shows that the conduction bands are primarily composed of La states while the valence bands are Te derived. This is intuitive (electron conduction on positive La sites as opposed to negative Te sites) and is consistent with previous calculations on La_3S_4.[12] The coupling of n and x (vacancy concentration) thus complicates both experimental and theoretical studies of electron transport within this class of materials.

The heavy bands lead to an increase in the energy dependence of the density of states $N(E)$, which can be observed in Fig. 2 at approximately −0.16 eV. This band feature is similarly reflected in the first-principles Hall carrier concentration (n_H), which is shown in the inset of Fig. 2. The n_H results are for 300 K, and the location of heavy-band minima are presented. The first-principles n_H values are slightly less than the corresponding values of the chemical n due to the nonparabolic nature of the bands. The deviation is largest at high energy (high n), where a maximum difference of 4% is observed at 300 K; a larger deviation is observed at higher T.

The optimum carrier concentration for thermoelectric application is experimentally determined to be $n_H \sim 9 \times 10^{20}$ cm^{-3},[7] which corresponds to energies where the heavy bands increase $N(E)$. Such a result makes physical sense, as an increase in the energy dependence of $N(E)$ is expected to increase $|\alpha|$ [see Eq. (1)]. At 300 K, the multiband features control the value of the optimum doping level; at higher T the effect is still present but is smeared out by temperature broadening of the Fermi functions.

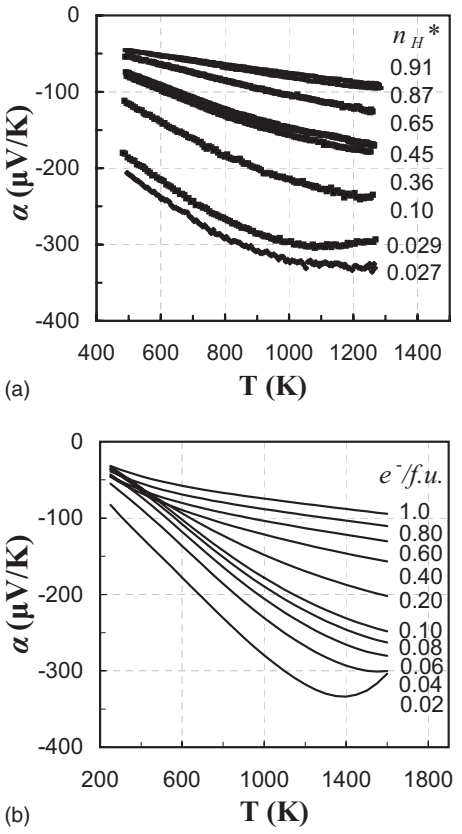

FIG. 3. Similar temperature dependence of the (a) experimental (Ref. 7) and (b) theoretical Seebeck coefficients is observed. Doping levels are indicated by (a) $n_H^*=n_H/4.49\times10^{21}$ cm^{-3} and (b) e^-/f.u. Note that at 300 K, e^-/f.u.$=n_H^*$: 1=0.96, 0.80=0.77, 0.60=0.59, 0.40=0.38, 0.20=0.17, 0.10=0.09, 0.08=0.07, 0.06=0.05, 0.04=0.04, and 0.02=0.02.

The impact of band structure on α is now examined in the context of experimental results. Behavior typical of a heavily doped semiconductor is observed for the electronic transport properties.[7] This is exemplified via the Seebeck coefficient: $|\alpha|$ increases linearly with T for all n at low T, at moderately high T degeneracy is lost for intermediate doping levels and the T dependence weakens, and for small n the detrimental effect of minority carriers can be observed at high T. These trends are observed in both the experimental [Fig. 3(a)][7] and theoretical [Fig. 3(b)] results. Heavily doped semiconductor behavior was also observed (experimentally) for σ, which decreases with increasing T due to decreasing electron mobility (μ) for $n_H>1\times10^{20}$ cm^{-3}.

Unusual carrier concentration dependence is observed for $|\alpha|$ in Fig. 4, where experimental data are compared to several models. The single parabolic band models (gray curves labeled by m^*/m_e) fail to accurately describe the experimentally determined dependence of α on n, and a more complicated model is required. While the α versus n curves calculated from the LDA band structure (red curves) are not in quantitative agreement with the experimental data, they do highlight the trend for a relative increase in the dependence of $|\alpha|$ on n near $n_H=1\times10^{21}$ cm^{-3}. Figure 4 contains data at 400 K and the inset is for 1000 K.

The crossing of theoretical α vs T curves in Fig. 3(b) is not possible within a single parabolic band framework, and

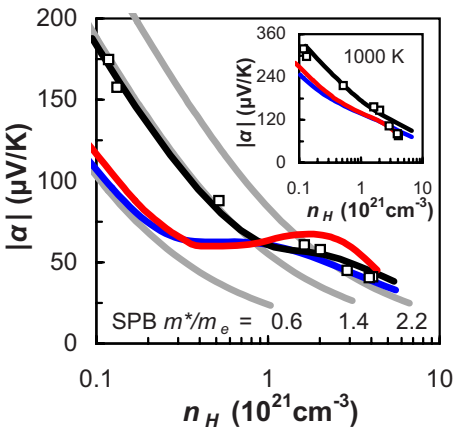

FIG. 4. (Color online) The experimental Seebeck coefficient at 400 K (open markers) is compared to several models, while the inset shows similar data for 1000 K. Single-band (SPB) models (gray curves with m^*/m_e indicated) fail to describe the experimental data. The *ab initio* calculations (red curves) demonstrate a relative increase in $|\alpha|$ at moderately high n, as does the multiparabolic band model utilizing *ab initio* parameters as input (blue curve). A semiempirical multiparabolic model (black curve) is generated using $m_1^*/m_e=0.844$, with all other parameters identical to those used in the blue curve; at 1000 K the black curve utilizes $m_1^*/m_e=1.13$.

this feature is highlighted by the red curve in Fig. 4. This n dependence makes sense in light of Eq. (1), from which we infer that the heavy degenerate bands increase $|\alpha|$ by increasing the energy dependence of $N(E)$. In a multiband system one should consider the contribution from each band, in which case one could say that the favorable effects of band edges are realized. From either perspective, the heavy bands clearly promote a relative increase in $|\alpha|$. This effect is most pronounced at lower T, but is present to some extent for all T examined. The agreement between experimental data and the *ab initio* results is best at high T, as highlighted by the inset of Fig. 4 which shows data for 1000 K. This suggests that either the band masses or CRTA is more applicable at high T.

Figure 4(a) also shows a multiparabolic band approximation of the first-principles results (blue curve). This curve was generated using Eqs. (2) and (3), with parameters (m_i^*, g_i) from the *ab initio* calculations as input. The multiparabolic band approximation of $|\alpha|$ agrees very well with the full calculation, indicating that minor asymmetries and band splitting do not have significant impact on α while multiband effects have dramatic impact on α. The parabolic band calculations are performed within the CRTA using common solutions to the Boltzmann transport equations,

$$\alpha=\frac{k_b}{q}\frac{\sum_i g_i\sqrt{m_i}\int_{E_{\min,i}}^{\infty}\left(-\frac{\partial f}{\partial\varepsilon}\right)(\varepsilon-E_{\min,i})^{3/2}(\varepsilon-\eta)d\varepsilon}{\sum_i g_i\sqrt{m_i}\int_{E_{\min,i}}^{\infty}\left(-\frac{\partial f}{\partial\varepsilon}\right)(\varepsilon-E_{\min,i})^{3/2}d\varepsilon}, \tag{2}$$

where f is the Fermi distribution function, and η, ε, and $E_{\min,i}$ are the reduced electrochemical potential, particle en-

ergy, and band minimum, respectively. The corresponding n values are

$$n = \left(\frac{4}{\sqrt{\pi}}\right)\left(\frac{2\pi k_b T}{h^2}\right)^{3/2} \sum_i g_i (m_i^*)^{3/2} \int_{E_{\min,i}}^{\infty} \varepsilon^{1/2} f d\varepsilon. \quad (3)$$

The final curve shown in Fig. 4(a) is a semiempirical multiparabolic band model (black curve). The semiempirical model was calculated using Eqs. (2) and (3) by allowing the value of m_1^* to be adjusted for a better description of the low-n_H data; all other band parameters remained constant. The agreement between the semiempirical model and the experimental data is quantitative at low T. However, the quantitative description fails as T increases and a larger m_1^* is required to describe the low-n data. Therefore, such a model is not a physical description of the system.

A better description of the transport would account for multiple scattering mechanisms, because both vacancies and phonons are likely to scatter electrons. If vacancies scatter electrons similar to ionized impurities, then the presence of vacancies would promote $\tau \propto \varepsilon^{3/2}$ behavior; acoustic phonon scattering of electrons has $\tau \propto \varepsilon^{-1/2}$ behavior. In this case, the dominant scattering mechanism would vary with T and one would expect the CRTA to be more accurate at high T (where phonon scattering dominates). While this is consistent with the results presented here, the electrical resistivity seems to suggest that μ is still mainly dominated by phonon scattering. At this level of analysis, it is most appropriate to say that either the density-functional band masses or the CRTA is not valid for all n and T examined.

The absolute effect of band features on zT is generally difficult to quantify, especially at high T where thermal energy influences energy scales and occupations, as well as carrier activation. However, an estimate can be made based on the extrapolation of the transport from lower carrier concentrations. This procedure reveals that at 1000 K the heavy bands increase zT by $\sim$20% at the optimum doping level of 9×10^{20} cm^{-3}. We note that due to the coupling of μ and m^*, as well as the use of the CRTA, it is very difficult to accurately quantify such hypothetical zT values. Nonetheless, this work strongly suggests that heavy bands lead to large thermoelectric performance in $La_{3-x}Te_4$ at moderately high n_H. This does not prove whether the presence of the light band is beneficial or detrimental. While it reduces $|\alpha|$, especially at low carrier concentrations, it does provide a pathway for the heavier electrons and therefore may be crucial for making the disordered $La_{3-x}Te_4$ system conductive.

In summary, the band structure of $La_{3-x}Te_4$ is found to have significant impact on its thermoelectric properties. This compound exploits a favorable increase in the density of states to produce a relatively large $|\alpha|$ at high doping levels. The relative increase in $|\alpha|$, combined with favorable thermal conductivity, yields a bulk n-type material with thermoelectric performance greater than that of current state of the art materials for $T > 1000$ K. This work demonstrates the importance of band structure calculations when considering electron transport, specifically the optimum doping level for thermoelectric application. Furthermore, this work highlights one type of band structure (light band/heavy band) that can lead to high thermoelectric efficiency.

ACKNOWLEDGMENTS

Work at ORNL was supported by the Department of Energy, EERE, Vehicle Technologies Program. The collection of experimental data and the subsequent analysis and calculations were performed at the Jet Propulsion Laboratory, California Institute of Technology under a contract with the National Aeronautics and Space Administration.

[1] M. Cutler and N. F. Mott, Phys. Rev. **181**, 1336 (1969).
[2] A. H. Wilson, *The Theory of Metals* (Cambridge University Press, Cambridge, England, 1953).
[3] G. D. Mahan, Solid State Phys. **51**, 81 (1998).
[4] J. P. Heremans *et al.*, Science **321**, 554 (2008).
[5] D. Bilc, S. D. Mahanti, K. F. Hsu, E. Quarez, R. Pcionek, and M. G. Kanatzidis, Phys. Rev. Lett. **93**, 146403 (2004).
[6] L. R. Danielson *et al.*, 7th International Conference on Thermoelectric Energy Conversion, Arlington, TX, 1988 (unpublished).
[7] A. F. May, J. P. Fleurial, and G. J. Snyder, Phys. Rev. B **78**, 125205 (2008).
[8] D. J. Singh and L. Nordstrom, *Planewaves, Pseudopotentials and the LAPW Method* (Springer, Berlin, 2006).
[9] P. Blaha *et al.*, http://www.wien2k.at
[10] P. J. Flahaut *et al.*, Acta Crystallogr. **19**, 14 (1965).
[11] G. K. H. Madsen and D. J. Singh, Comput. Phys. Commun. **175**, 67 (2006).
[12] J. H. Shim *et al.*, Physica B **328**, 148 (2003).